Interdiffusion in α solid solutions of the Cu–Zn–Sn system

TOMOSHI TAKAHASHI, MICHITOMO KATO
*Department of Metallurgical Engineering, Niihama National College of Technology,
7-1 Yagumo, Niihama, Ehime 792, Japan*

YORITOSHI MINAMINO, TOSHIMI YAMANE
*Department of Materials Science and Engineering, Faculty of Engineering, Osaka University,
2-1 Yamadaoka, Suita, Osaka 565, Japan*

The interdiffusion coefficients in the α fcc phase of Cu–Zn–Sn alloys, $\tilde{D}^{Cu}_{SnSn}$, $\tilde{D}^{Cu}_{SnZn}$, $\tilde{D}^{Cu}_{ZnZn}$ and $\tilde{D}^{Cu}_{ZnSn}$, have been determined at 1073 K. The concentration profiles indicate that the diffusion rate of tin is greater than that of zinc in the Cu–Zn–Sn alloy. The diffusion paths show the typical S-shaped curves. All of the four interdiffusion coefficients are positive and they are very sensitive to the solute concentration. The atomic mobilities of the three diffusing elements in Kirkendall planes increase in the order of Cu, Zn, Sn. The interaction energy of the Cu–Sn bond is much larger than that of the Zn–Sn bond. From the results of the present work it seems that the Onsager reciprocal relation holds in the α phase of the Cu–Zn–Sn system.

1. Introduction

Copper-rich alloys in the Cu–Zn–Sn system are a kind of commercial alloys which have high strength, wear and corrosion resistances and are used for bronze casting in mechanical industries [1]. Diffusion in the alloys has become an important subject of investigation to obtain basic information on heat treatments and oxidation, etc. [2, 3]. Investigations of interdiffusion in Cu–Zn–Sn alloys have been performed by Rhines *et al.* [4], Kirkaldy *et al.* [5] and Dayananda *et al.* [6]. However, the interdiffusion coefficients of Cu–Zn–Sn alloys at 1073 K have not been determined, and verification of the Onsager reciprocal relation has not been attempted in the present system.

The purposes of the present work are (a) to determine the ternary interdiffusion coefficients in the α-phase region of the Cu–Zn–Sn system at 1073 K by use of the solid–solid couples, (b) to estimate the interaction parameters in Cu–Zn–Sn alloys from the interdiffusion coefficients, and (c) to verify the Onsager reciprocal relation for this system.

2. Experimental procedure

A constitution diagram [7] of the copper side of the Cu–Zn–Sn system at 873 K is shown in Fig. 1. Terminal compositions of diffusion couples are listed in Table I. Nineteen diffusion couples were prepared in order to determine the interdiffusion coefficients in the α-phase field of this system. The diffusion couples C1 and C2 were couples for binary diffusion in the Cu–Zn system and D1–D4 were couples for binary diffusion in the Cu–Sn system. Cu–Zn, Cu–Sn and α-Cu–Zn–Sn alloys of selected compositions were prepared from 99.99 wt % Cu, 99.99 wt % Zn and 99.9 wt % Sn in an induction melting furnace in an

argon atmosphere. The alloy ingots were annealed at temperatures 50 to 70 K below their melting points for 604.8 ksec, in order to establish the homogenization and grain growth. The grain diameter of these alloys was more than about 1 mm.

The Cu–Zn and α-Cu–Zn–Sn alloys were turned to rods of diameter 8 mm and length 80 mm by a lathe. A hole of the same dimensions was drilled in blocks of pure copper and the Cu–Sn alloys (25 mm × 25 mm × 70 mm). The faces of the rod alloys and the holes in the blocks were mechanically polished by 4/0 emery paper (600 grade), and then washed with acetone. The alloy rods were then inserted into the holes in the blocks. These combined metals were quickly (within about 180 sec) rolled to 70% reduction in thickness after heating at 1073 K for 3.6 ksec, and then quenched in water. The rolling has the advantage that the oxide film at the interface between the metals is broken up and distributed over a much larger area [8]. The rolled metals were cut into 5 mm widths as the diffusion couples. The interfaces of the diffusion couples were examined by a Jeol JXA-733 electron probe microanalyser (EPMA). It was found that diffusion during the welding treatments was negligible.

The diffusion couples were annealed at 1073 K for 74.8 ksec under a purified argon atmosphere of about 10^5 Pa in order to prevent oxidation of the diffusion couples and evaporation of zinc. After the diffusion annealing, the couples were quenched in ice-water. The annealed couples were metallographically polished along planes parallel to the diffusion direction. Solute concentration profiles in these diffusion couples were measured by EPMA. The characteristic X-ray intensities of zinc and tin were corrected for atomic number, absorption and fluorescence effects and
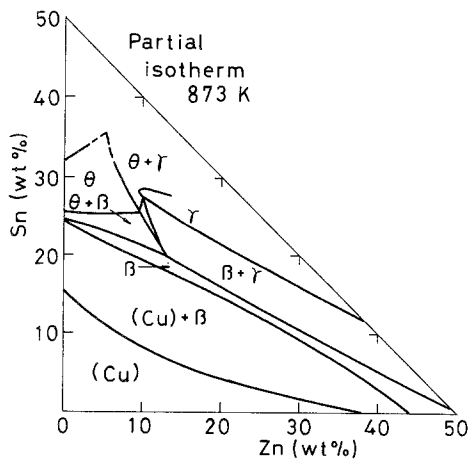
Figure 1 Constitution diagram of the copper side of the Cu–Zn–Sn system.

TABLE I Terminal compositions of diffusion couples

Couple name	Composition (at %)
A1	Cu/Cu– 2.4Zn–6.2Sn
A2	Cu/Cu– 5.5Zn–5.3Sn
A3	Cu/Cu–10.1Zn–4.3Sn
A4	Cu/Cu–14.4Zn–2.3Sn
B1	Cu– 4.7Zn/Cu–2.7Sn
B2	Cu– 8.0Zn/Cu–4.1Sn
B3	Cu–13.0Zn/Cu–5.5Sn
B4	Cu– 8.0Zn/Cu–6.9Sn
B5	Cu–13.0Zn/Cu–6.9Sn
B6	Cu–17.7Zn/Cu–6.9Sn
B7	Cu– 4.7Zn/Cu–6.9Sn
B8	Cu– 8.0Zn/Cu–2.7Sn
B9	Cu–17.7Zn/Cu–5.5Sn
C1	Cu/Cu–24.6Zn
C2	Cu/Cu–28.5Zn
D1	Cu/Cu– 2.7Sn
D2	Cu/Cu– 4.1Sn
D3	Cu/Cu– 5.5Sn
D4	Cu/Cu– 6.9Sn

converted into concentration values of zinc and tin using the bulk alloy compositions at the ends of the couples as standards [9, 10].

Interdiffusion in a ternary alloy 1–2–3 is expressed by an extended Fick's second law on the basis of Matano coordinates:

$$\frac{\partial C_1}{\partial t} = \frac{\partial}{\partial x}\left(\tilde{D}_{11}^3 \frac{\partial C_1}{\partial x}\right) + \frac{\partial}{\partial x}\left(\tilde{D}_{12}^3 \frac{\partial C_2}{\partial x}\right) \quad (1)$$

and

$$\frac{\partial C_2}{\partial t} = \frac{\partial}{\partial x}\left(\tilde{D}_{21}^3 \frac{\partial C_1}{\partial x}\right) + \frac{\partial}{\partial x}\left(\tilde{D}_{22}^3 \frac{\partial C_2}{\partial x}\right) \quad (2)$$

where C_1 and C_2 are the concentrations of Solutes 1 and 2, t is the diffusion time and x the distance from the Matano interface. Constituent 3 (denoted by a superscript) represents the solvent and is treated as a dependent variable [11]. The interdiffusion coefficients $\tilde{D}_{11}^3$ and $\tilde{D}_{22}^3$ are referred to as the 'direct" or "major" coefficients, and $\tilde{D}_{12}^3$ and $\tilde{D}_{21}^3$ as the "indirect" or "cross" coefficients. In this study, the solvent is copper and solutes 1 and 2 are tin and zinc, respectively.

Kirkaldy *et al.* [12] have shown that Equations 1 and 2 can be solved by an extension of the Boltzmann–Matano method to ternary equations:

$$\int_{C_1^{-\infty}}^{C_1} x\,dC_1 = -2t\left(\tilde{D}_{11}^3 \frac{\partial C_1}{\partial x} + \tilde{D}_{12}^3 \frac{\partial C_2}{\partial x}\right) \quad (3)$$

and

$$\int_{C_2^{-\infty}}^{C_2} x\,dC_2 = -2t\left(\tilde{D}_{21}^3 \frac{\partial C_1}{\partial x} + \tilde{D}_{22}^3 \frac{\partial C_2}{\partial x}\right) \quad (4)$$

and the origin for x must be chosen in such a way that

$$\int_{C_1^{-\infty}}^{C_1^{+\infty}} x\,dC_1 = \int_{C_2^{-\infty}}^{C_2^{+\infty}} x\,dC_2 = 0 \quad (5)$$

where $C_i^{-\infty}$ and $C_i^{+\infty}$ ($i = 1, 2$) are the terminal compositions at the ends of the diffusion couples. The four interdiffusion coefficients in Equations 3 and 4 are evaluated at the common compositions (C_1 and C_2) of intersection of the diffusion paths. The binary Cu–Zn and Cu–Sn interdiffusion coefficients were determined by using the Matano method [13].

3. Results and discussion
3.1. Concentration profiles, interdiffusion fluxes and diffusion paths

Typical concentration profiles of the couples A1 and B7 annealed at 1073 K are shown in Figs 2a and b, respectively. The origin of the abscissa in Figs 2a and b is the Matano interface. The diffusion distances of tin are larger than those of zinc. The concentration profiles indicate that the diffusion rate of tin is greater than that of zinc in Cu–Zn–Sn alloys.

For uniaxial diffusion in the ternary system, the interdiffusion flux $\tilde{J}_{Zn}$ [14] is represented by

$$\tilde{J}_{Zn} = \tilde{J}_{ZnZn} + \tilde{J}_{ZnSn}$$

$$= -\tilde{D}_{ZnZn}^{Cu}\frac{\partial C_{Zn}}{\partial x} - \tilde{D}_{ZnSn}^{Cu}\frac{\partial C_{Sn}}{\partial x} \quad (6)$$

where $\tilde{J}_{ZnZn}$ is the direct flux of zinc due to the zinc concentration gradient and $\tilde{J}_{ZnSn}$ is the indirect flux of zinc due to the tin concentration. A similar relation holds for $\tilde{J}_{Sn}$. Fig. 3 shows the relation between $\tilde{J}_{ZnSn}/\tilde{J}_{ZnZn}$ and tin concentration for the couples A1 to A4. The influence of the indirect flux becomes larger with an increase of tin concentration.

The diffusion paths for the diffusion couples are shown in Fig. 4. The couple names are also written in Fig. 4. In the Cu–Zn–Sn system, the alloying constituents do not diffuse linearly on the ternary isotherm at 1073 K. The diffusion paths show the typical S-shaped curves. The formation of S-shaped diffusion paths is attributed to the magnitude of the difference between the diffusion rates of zinc and tin (see Figs 2a and b) and the presence of a marked interaction between the diffusing elements. S-shaped diffusion paths are obtained in the Cu–Ni–Zn [15, 16], Al–Ag–Zn [17], Cu–Mn–Zn [18] and Cu–Ni–Sn [19] systems.

3.2. Diffusion coefficients

Reports of the lattice parameters in Cu–Zn–Sn alloys [20] indicate that the partial molar volumes of these alloys are constant in the concentration range of the
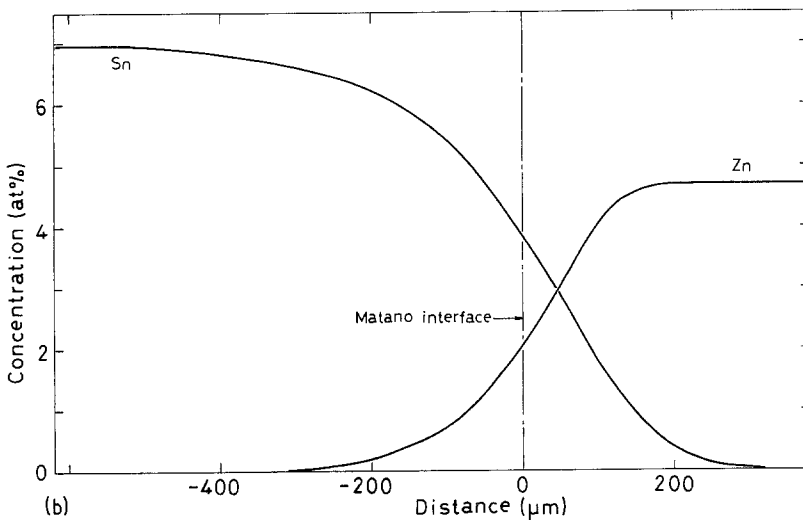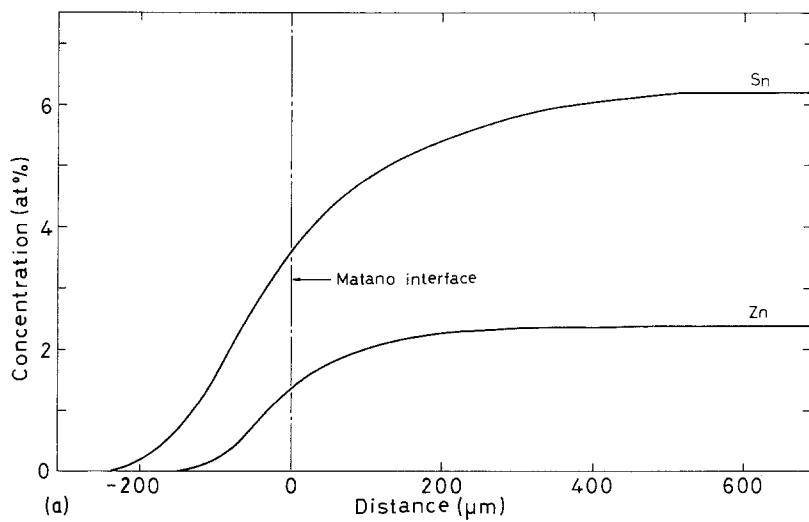
Figure 2 Typical concentration profiles of zinc and tin for diffusion couples (a) A1 and (b) B7 annealed at 1073 K for 74.83 ksec.

present work. Furthermore, since the molar volumes do not vary markedly with composition [20], the volume change in the diffusion zone is negligible. Therefore, Equations 3 to 5 can be applied to the Cu–Zn–Sn system. The interdiffusion coefficients $\tilde{D}_{SnSn}^{Cu}$, $\tilde{D}_{SnZn}^{Cu}$, $\tilde{D}_{ZnZn}^{Cu}$ and $\tilde{D}_{ZnSn}^{Cu}$ are evaluated at the composition points of intersection of diffusion paths by using Equations 3 to 5.

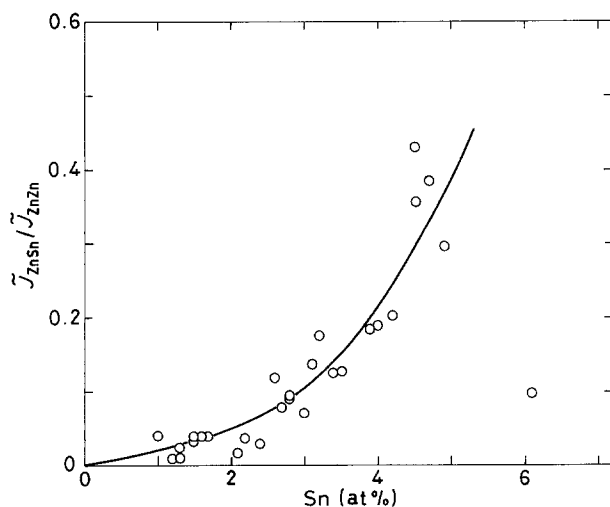The values of the four diffusion coefficients at

1073 K are listed in Table II and are shown in Figs 5a to d. Isodiffusion coefficient contours are shown by the broken lines. The values of $\tilde{D}_{SnSn}^{Cu}$, $\tilde{D}_{SnZn}^{Cu}$, $\tilde{D}_{ZnZn}^{Cu}$ and $\tilde{D}_{ZnSn}^{Cu}$ are very sensitive to the solute concentrations. The values of $\tilde{D}_{SnSn}^{Cu}$ and $\tilde{D}_{SnZn}^{Cu}$ increase towards the tin-rich corner, and those of $\tilde{D}_{ZnZn}^{Cu}$ and $\tilde{D}_{ZnSn}^{Cu}$ increase towards the zinc-rich corner. Diffusion coefficients of pure metals and binary alloys are related to their
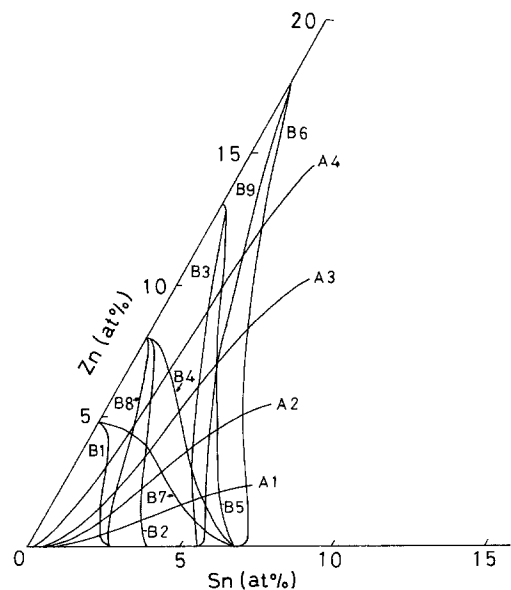

Figure 3 Relation between $\tilde{J}_{ZnSn}/\tilde{J}_{ZnZn}$ and tin concentration for diffusion couples A1 to A4 at 1073 K.

Figure 4 Diffusion paths for diffusion couples annealed at 1073 K.

3196

Diffusion couple	Composition (at %)		Interdiffusion coefficients ($10^{-14}\,m^2\,sec^{-1}$)			
	Zn	Sn	$\tilde{D}^{Cu}_{SnSn}$	$\tilde{D}^{Cu}_{SnZn}$	$\tilde{D}^{Cu}_{ZnZn}$	$\tilde{D}^{Cu}_{ZnSn}$
A1–B1	0.47	2.2	9.7	0.12	3.4	−0.25
A1–B2	1.1	3.2	12	2.5	4.2	0.51
A1–B3	1.9	4.5	20	7.7	8.4	1.5
A1–B4	2.0	4.7	22	9.6	9.3	1.8
A1–B5	2.2	5.2	27	6.3	11	2.1
A1–B6	2.3	6.1	18	6.2	16	4.1
A1–B7	1.7	4.2	18	2.7	8.3	0.83
A1–B8	0.58	2.4	8.9	1.9	3.8	−0.34
A1–B9	2.1	4.9	26	9.1	10	1.6
A2–B1	0.95	1.9	9.8	0.095	3.3	−0.57
A2–B2	2.3	2.7	11	1.9	4.5	0.66
A2–B3	3.9	3.5	16	4.0	7.6	1.7
A2–B4	3.7	3.4	16	3.5	7.0	1.6
A2–B5	4.6	4.0	21	4.7	11	2.4
A2–B6	5.1	4.5	27	8.8	14	4.3
A2–B7	2.9	3.0	15	1.8	6.0	0.81
A2–B8	1.2	2.1	9.3	1.1	3.5	−0.41
A2–B9	4.4	3.9	18	4.7	9.8	2.2
A3–B1	1.5	1.7	10	0.64	3.1	−0.039
A3–B2	3.5	2.1	11	1.9	4.6	0.42
A3–B3	6.1	2.6	16	3.3	8.3	4.5
A3–B4	5.2	2.4	13	2.8	6.7	1.1
A3–B5	6.9	2.8	20	3.4	10	3.9
A3–B6	8.3	3.1	24	5.3	14	5.9
A3–B7	3.7	2.2	12	1.8	4.7	0.94
A3–B8	2.1	1.8	11	1.2	3.6	−0.38
A3–B9	7.1	2.8	19	4.0	10	4.3
A4–B1	3.1	1.0	8.9	0.32	3.0	1.0
A4–B2	5.7	1.3	10	0.87	4.7	1.7
A4 B3	9.0	1.5	14	1.5	8.4	4.8
A4–B4	6.8	1.3	10	1.1	5.8	0.89
A4–B5	9.8	1.5	16	1.6	9.4	3.8
A4–B6	12	1.7	18	2.8	13	4.7
A4–B7	4.5	1.2	9.7	0.62	3.9	0.47
A4–B8	4.6	1.2	9.2	0.70	4.1	−0.30
A4–B9	11	1.6	16	2.3	11	4.9
B2–B7	3.9	1.9	12	2.4	4.6	0.96
B3–B4	2.9	4.0	18	4.6	7.3	0.48
B4–B9	1.6	5.1	22	9.0	11	2.7
B7–B8	4.4	1.3	9.9	0.87	4.2	0.69

melting points, etc. [21–23] and the tendency of the magnitude of the diffusion coefficients in ternary Cu–Zn–Sn alloys corresponds to the direction of decrease of the liquidus temperature [24]. Almost all the direct and indirect coefficients at the same composition reveal the relations $\tilde{D}^{Cu}_{SnSn} > \tilde{D}^{Cu}_{ZnZn} > 0$ and $\tilde{D}^{Cu}_{SnZn} > \tilde{D}^{Cu}_{ZnSn} > 0$ in the phase region. The thermodynamic conditions for the four interdiffusion coefficients have been presented as follows [25, 26]:

$$\tilde{D}^3_{11} > 0 \qquad \tilde{D}^3_{22} > 0 \qquad \tilde{D}^3_{12}\tilde{D}^3_{21} > 0 \qquad (7)$$

and

$$\tilde{D}^3_{11}\tilde{D}^3_{22} - \tilde{D}^3_{12}\tilde{D}^3_{21} > 0 \qquad (8)$$

These relations are satisfied by the experimental values of the present work except for the negative values of indirect coefficients, which appear in the neighbourhood of the terminal composition. While the values of $\tilde{D}^3_{12}$ and $\tilde{D}^3_{21}$ should have the same signs as shown in Equation 7, the negative values of $\tilde{D}^{Cu}_{ZnSn}$ are liable to be induced in the vicinity of the terminal compositions as already reported [27, 28].

The limiting values of the interdiffusion coefficients on the sides of the ternary i–j–k diagram have been

established by Shuck and Tool [29]. The limiting values of the direct coefficients $\tilde{D}^k_{ii}$ are

$$\lim_{C_j \to 0} \tilde{D}^k_{ii} = \tilde{D}_{i-k} \qquad (9)$$

on the i–k side, where $\tilde{D}_{i-k}$ is the diffusion coefficient of the binary i–k system. The direct coefficients $\tilde{D}^{Cu}_{SnSn}$ and $\tilde{D}^{Cu}_{ZnZn}$ approach the binary coefficients $\tilde{D}_{Cu-Sn}$ and $\tilde{D}_{Cu-Zn}$ on the Cu–Sn and Cu–Zn sides in Figs 5a and c. The limiting values of the indirect coefficients $\tilde{D}^k_{ij}$ are

$$\lim_{C_j \to 0} \tilde{D}^k_{ij} = 0 \qquad (10)$$

on the j–k side. The indirect coefficients $\tilde{D}^{Cu}_{SnZn}$ and $\tilde{D}^{Cu}_{ZnSn}$ approach zero on the Cu–Zn and Cu–Sn sides, respectively, as shown in Figs 5b and d.

In addition, the limiting values of $\tilde{D}^k_{ii}$ are

$$\lim_{C_j \to 0} \tilde{D}^k_{ii} = D^*_{i(j-k)} \qquad (11)$$

on the j–k side, where $D^*_{i(j-k)}$ is the impurity diffusion coefficients of component i in a binary j–k alloy. The values of $D^*_{Sn(Cu-Zn)}$ and $D^*_{Zn(Cu-Sn)}$ can be determined by Hall's method [30, 31] at the terminal compositions of the profiles obtained from the diffusion couples B1 to B9. Results obtained at 1073 K are shown in Figs 5a
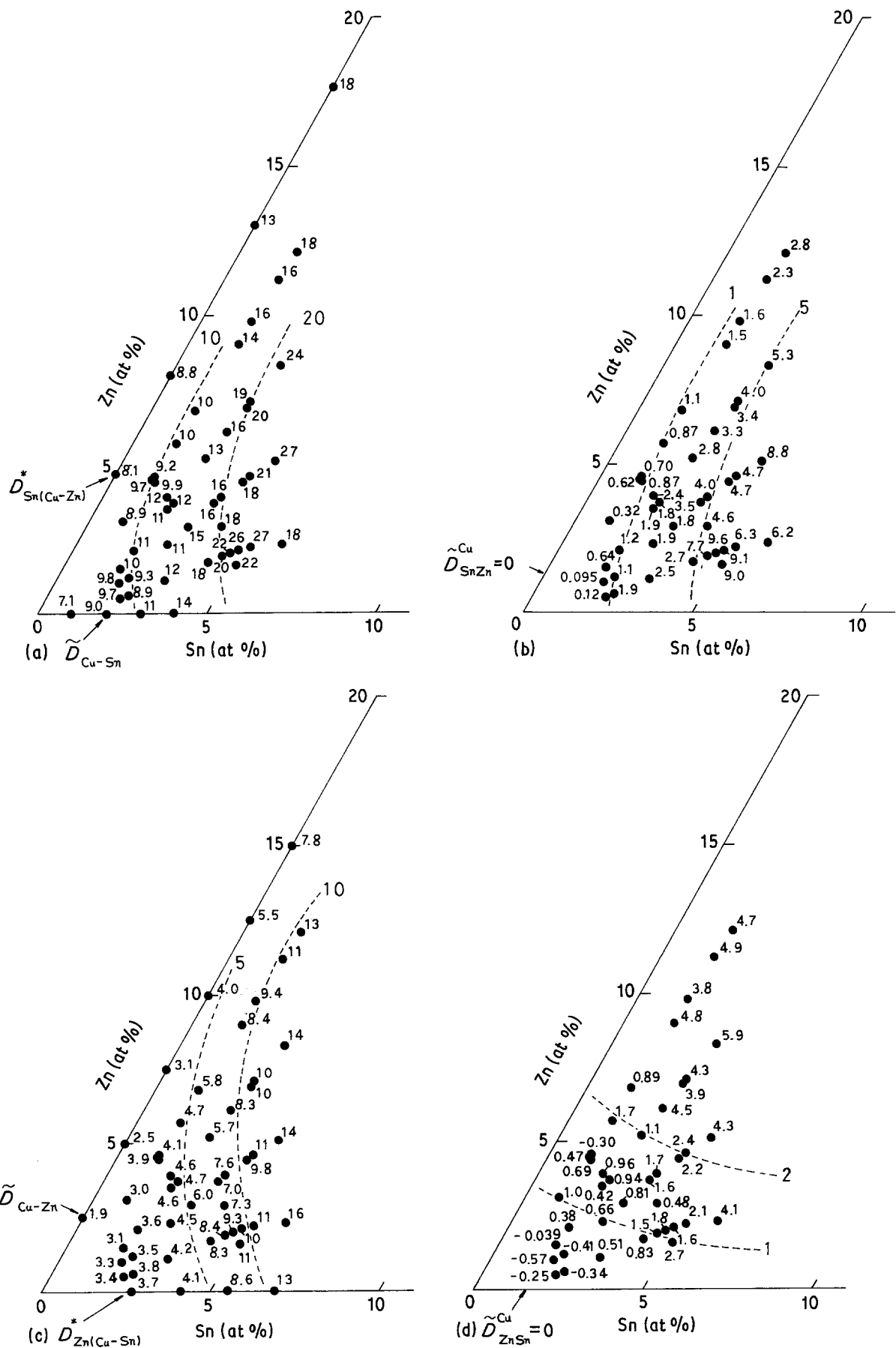
Figure 5 Direct and indirect interdiffusion coefficients (a) $\tilde{D}^{Cu}_{SnSn}$, (b) $\tilde{D}^{Cu}_{SnZn}$, (c) $\tilde{D}^{Cu}_{ZnZn}$ and (d) $\tilde{D}^{Cu}_{ZnSn}$. Units are $10^{-14} \, m^2 \, sec^{-1}$.

and c. The direct coefficients $\tilde{D}^{Cu}_{SnSn}$ on the Cu–Zn sides (Fig. 5a) correspond to the impurity diffusion coefficients of tin in the Cu–Zn alloys, $D^*_{Sn(Cu-Zn)}$. The direct coefficients $\tilde{D}^{Cu}_{ZnZn}$ on the Cu–Sn sides (Fig. 5c) correspond to the impurity diffusion coefficients of

zinc in the Cu–Sn alloys, $D^*_{Zn(Cu-Sn)}$. The values of $D^*_{Sn(Cu-Zn)}$ and $D^*_{Zn(Cu-Sn)}$ at 1073 K are also shown in Fig. 6 with those of $\tilde{D}_{Cu-Zn}$ and $\tilde{D}_{Cu-Sn}$. The concentration dependence of $D^*_{Zn(Cu-Sn)}$ and $\tilde{D}_{Cu-Sn}$ are more marked than those of $D^*_{Sn(Cu-Zn)}$ and $\tilde{D}_{Cu-Zn}$, since the
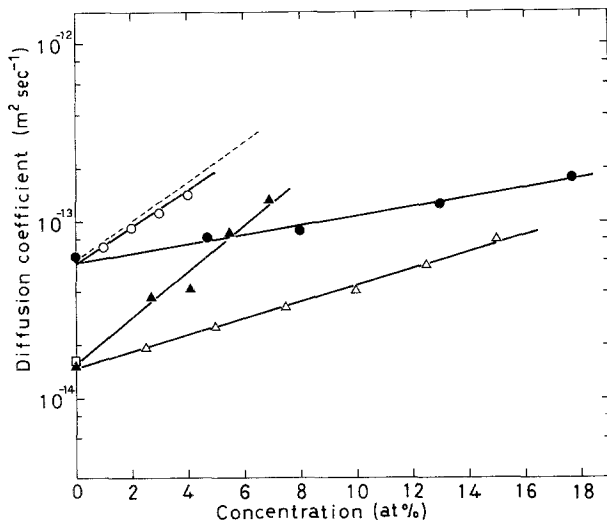
Figure 6 Variation of (▲) $D^*_{Zn(Cu-Sn)}$, (●) $D^*_{Sn(Cu-Zn)}$, (○) $\tilde{D}_{Cu-Sn}$ and (△) $\tilde{D}_{Cu-Zn}$ with concentration at 1073 K. (---) $\tilde{D}_{Cu-Sn}$ from Hoshino *et al.* [33]; (□) $D^*_{Zn(Cu)}$ from Anusavice and DeHoff [34].

gradient of the liquidus line of the copper side in the Cu–Sn system is much larger than that of the copper side in the Cu–Zn system [32]; that is, $D^*_{Zn(Cu-Sn)}$ and $\tilde{D}_{Cu-Sn}$ approach the liquidus line at lower solute concentrations. The values of $\tilde{D}_{Cu-Sn}$ and $D^*_{Zn(Cu)}$ are in good agreement with literature data [33, 34].

3.3. Atomic mobilities

The atomic mobility β_i [35] of component i at the composition of the plane of Kirkendall markers is given by

$$\beta_i = -\frac{A_i}{\left(2tC_i \dfrac{\partial \mu_i}{\partial x} \dfrac{1}{N_0}\right)} \quad (i = 1, 2, \dots n) \quad (12)$$

where A_i and C_i refer, respectively, to the cumulative intrinsic flux and molar concentration, $\partial \mu_i / \partial x$ is the gradient of its chemical potential, and N_0 is Avogadro's number. In the range of validity of Henry's law, $\partial \mu_i / \partial x$ is represented by

$$\frac{\partial \mu_i}{\partial x} = \frac{RT}{C_i} \frac{\partial C_i}{\partial x} \quad (13)$$

where R is the gas constant and T the diffusion temperature. The use of Equation 13 in Equation 12 yields

$$\beta_i = -\frac{A_i}{\left(2tRT \dfrac{\partial C_i}{\partial x} \dfrac{1}{N_0}\right)} \quad (14)$$

Table III presents the mobilities of the three diffusing species at the compositions of the planes of Kirkendall

markers. The mobilities of α-Cu–Zn–Sn alloys increase in the order Cu, Zn, Sn.

3.4. Interaction parameters and the Onsager reciprocal relation

Kirkaldy *et al.* [36] have derived the relation between $\tilde{D}^3_{ij}/\tilde{D}^3_{ii}$ and Wagner's interaction parameter, $\varepsilon_i^{(i)}$ and $\varepsilon_i^{(j)}$:

$$\frac{\tilde{D}^3_{ij}}{\tilde{D}^3_{ii}} = \frac{N_i + N_i N_3 \varepsilon_i^{(j)}}{1 - N_j + N_i N_3 \varepsilon_i^{(i)}} \quad (15)$$

where N_i, N_j and N_3 are the atom fractions of Components i, j and 3, respectively. For highly dilute solutions, Equations 15 reduces to the relation

$$\tilde{D}^3_{ij}/\tilde{D}^3_{ii} = (1 + \varepsilon_i^{(j)})N_i \quad (16)$$

The interdiffusion coefficients in the ternary system can be described in a different form by the choice of dependent component or "solvent". The dependent component can be changed from superscript 3 (Cu) to 2 (Zn) by using Equations 17 to 20 [37]:

$$\tilde{D}^2_{11} = \tilde{D}^3_{11} - \frac{\bar{V}_1}{\bar{V}_2} \tilde{D}^3_{12} \quad (17)$$

$$\tilde{D}^2_{13} = -\frac{\bar{V}_3}{\bar{V}_2} \tilde{D}^3_{12} \quad (18)$$

$$\tilde{D}^2_{31} = -\frac{\bar{V}_1}{\bar{V}_3}\left(\tilde{D}^3_{22} - \tilde{D}^3_{11} + \frac{\bar{V}_1}{\bar{V}_2}\tilde{D}^3_{12} - \frac{\bar{V}_2}{\bar{V}_1}\tilde{D}^3_{21}\right) \quad (19)$$

$$\tilde{D}^2_{33} = \tilde{D}^3_{22} + \frac{\bar{V}_1}{\bar{V}_2}\tilde{D}^3_{12} \quad (20)$$

where $\bar{V}_1$, $\bar{V}_2$ and $\bar{V}_3$ are the partial molar volumes of 1, 2 and 3, respectively.

Fig. 7a shows the relation between $\tilde{D}^{Cu}_{SnZn}/\tilde{D}^{Cu}_{SnSn}$ and tin concentration. Similarly, Fig. 7b shows the relation for $\tilde{D}^{Zn}_{SnCu}/\tilde{D}^{Zn}_{SnSn}$ converted by Equations 17 and 18. The values of $\bar{V}_1$, $\bar{V}_2$ and $\bar{V}_3$ calculated from the data of the lattice parameter are 10.6, 8.47 and 7.11 × $10^{-6} \text{m}^3 \text{mol}^{-1}$, respectively [20]. The solid lines in Figs 7a and b are drawn for Equation 16 with the values of $\varepsilon^{(Zn)}_{Sn} = 6$ and $\varepsilon^{(Cu)}_{Sn} = -8.5$. The experimental values are distributed about these lines, and they satisfy Equation 16 in the dilute range from 0 to about 5 at % Sn. The positive values of $\tilde{D}^{Cu}_{SnZn}$ and $\tilde{D}^{Cu}_{ZnSn}$ indicate that the activities of tin and zinc are increased by zinc and tin, respectively. Since the interaction parameter $\varepsilon^{(Zn)}_{Sn}$ has a positive value, and $\varepsilon^{(Cu)}_{Sn}$ has a negative value, it is expected that the interaction energy of the Cu–Sn bond is much larger than the value for the Zn–Sn bond.

TABLE III Atomic mobilities in α-Cu–Zn–Sn alloys: present work (1073 K)

Diffusion couple	Composition (at %)		Atomic mobility ($10^7 \text{m sec}^{-1} \text{N}^{-1}$)		
	Zn	Sn	β_{Cu}	β_{Zn}	β_{Sn}
C1	17.5	0	0.61	1.2	–
D4	0	4.1	0.96	–	1.1
A1	1.8	4.3	0.90	1.4	2.2
A2	4.0	3.7	0.71	1.3	2.6

Figure 7 Relation between (a) $\tilde{D}^{Cu}_{SnZn}/\tilde{D}^{Cu}_{SnSn}$, (b) $\tilde{D}^{Zn}_{SnCu}/\tilde{D}^{Zn}_{SnSn}$ and tin concentration. 1073 K, 74.83 ksec.
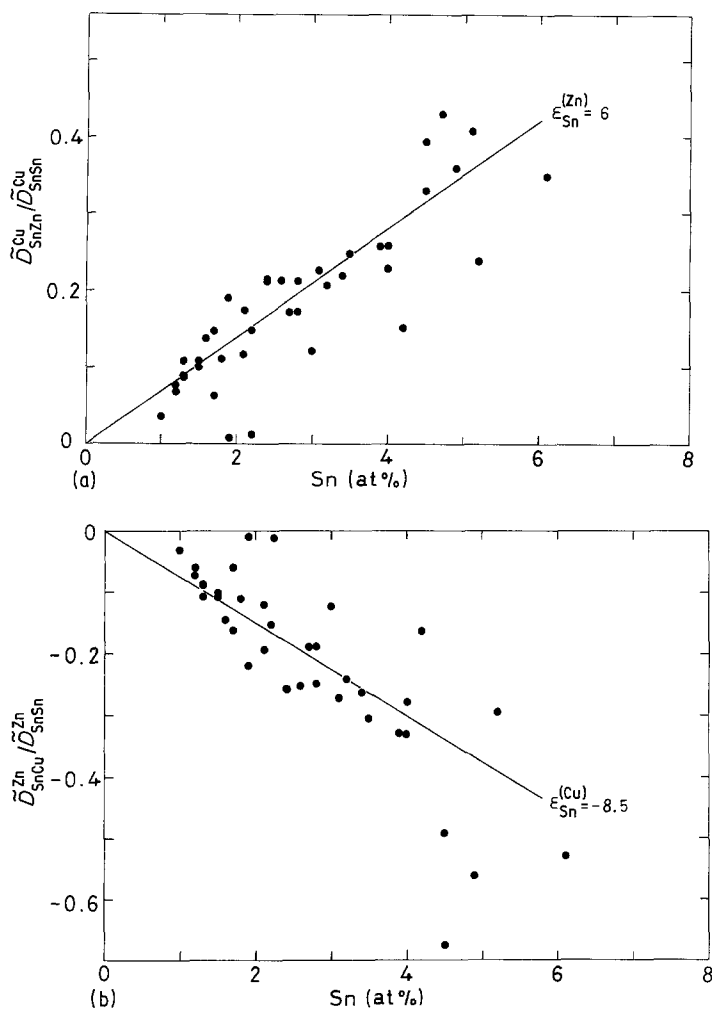
The Onsager reciprocal relation [38] for the inter-diffusion coefficients in the ternary system is given by

$$\left[g_{22} + (1 - N_2) \frac{1}{N_2} g_{12} \right] \tilde{D}^3_{11}$$

$$+ \left[(1 - N_1) \frac{1}{N_2} g_{22} + \frac{N_1}{N_2} g_{12} \right] \tilde{D}^3_{21}$$

$$= \left[g_{11} + (1 - N_1) \frac{1}{N_1} g_{21} \right] \tilde{D}^3_{22}$$

$$+ \left[(1 - N_2) \frac{1}{N_1} g_{11} + \frac{N_2}{N_1} g_{21} \right] \tilde{D}^3_{12} \quad (21)$$

The thermodynamic factors g_{11} and g_{12} are expressed by

$$g_{11} = \left(\frac{\partial \log a_1}{\partial \log N_1} \right)_{N_2}$$

$$= 1 + N_1 \frac{\partial \ln \gamma_1}{\partial N_1}$$

$$g_{11} = 1 + N_1 \varepsilon_1^{(1)} \quad (22)$$

and

$$g_{12} = \left(\frac{\partial \log a_1}{\partial \log N_2} \right)_{N_1}$$

$$= N_2 \frac{\partial \ln \gamma_1}{\partial N_2}$$

$$g_{12} = N_2 \varepsilon_1^{(2)} \quad (23)$$

where a_1 and γ_1 are the activity and activity coefficient of Component 1, respectively. Similar equations can be also derived for g_{22} and g_{21}. When the Onsager reciprocal relation is available in the α phase, the left-hand side of Equation 21 is in agreement with the right-hand side. Ratios of differences between the values of two sides, %Δ [39], can be evaluated by

$$\%\Delta = 100 \left| \frac{A - B}{(A + B)/2} \right| \quad (24)$$

where A is the left-hand side in Equation 21 and B is the right-hand one. As mentioned with Figs 7a and b, if Henry's law is valid in the α phase field of the Cu–Zn–Sn system, the value of $\varepsilon_{Sn}^{(Zn)}$ is equal to that of $\varepsilon_{Zn}^{(Sn)}$ and their values are 6, while both $\varepsilon_{Sn}^{(Sn)}$ and $\varepsilon_{Zn}^{(Zn)}$ are zero. The Onsager reciprocal relation can be evaluated by substituting the experimental values $\varepsilon_i^{(j)}$ and $\tilde{D}^3_{ij}$ ($i, j = 1, 2$) at each concentration mentioned above in Equation 21, and the results are shown in Fig. 8. The Onsager reciprocal relations in ternary alloys have been verified in Cu–Ag–Au [38], Ti–V–Zr [37] and Cu–Mn–Zn [18] systems. In the present work, the errors in the reported values are estimated to be within ±10% for the direct coefficients, ±20% for the indirect coefficients and 30% for the interaction parameters. The maximum relative errors in evaluating Equation 21 are about 50%. Almost all the values of %Δ are within 50% except for the five data (open circles) in the vicinity of the terminal compositions. The authors conclude that the Onsager reciprocal
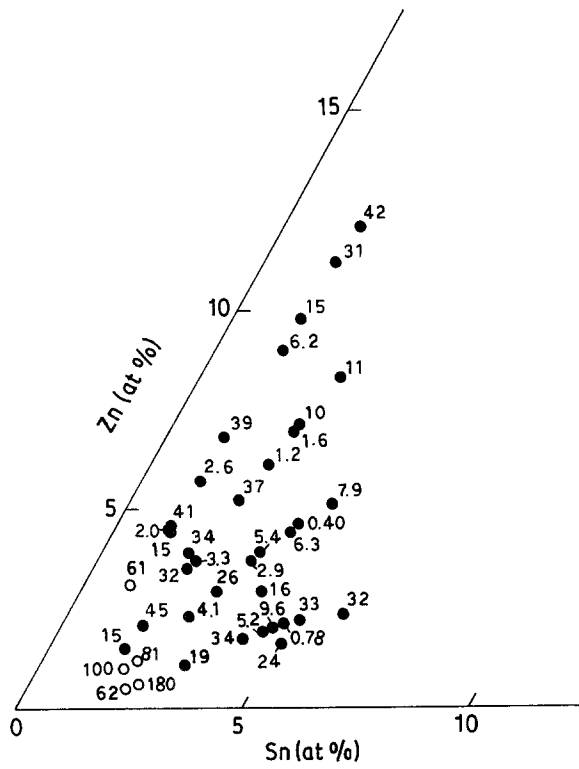
Figure 8 Discrepancy with Onsager relations, $\%\Delta = 100|2(A - B)/(A + B)|$ (Equation 24); ($\bullet$) $\%\Delta < 50\%$, ($\circ$) $\%\Delta > 50\%$.

relation is valid in the α phase field of the Cu–Zn–Sn system, since the values of $\%\Delta$ are smaller than the maximum relative errors and many experimental values of the two sides in Equation 21 agree with the deviations within 30%.

On the other hand, the phenomenological coefficients L_{ij} ($i, j = 1, 2$) [40] are related to the inter-diffusion coefficients and the thermodynamic factors by

$$L_{11} = \frac{d\tilde{D}_{11}^3 - b\tilde{D}_{12}^3}{ad - bc} \qquad L_{12} = \frac{a\tilde{D}_{12}^3 - c\tilde{D}_{11}^3}{ad - bc}$$

$$L_{21} = \frac{d\tilde{D}_{21}^3 - b\tilde{D}_{22}^3}{ad - bc} \qquad L_{22} = \frac{a\tilde{D}_{22}^3 - c\tilde{D}_{21}^3}{ad - bc}$$

(25)

where

$$a = \left(1 + \frac{C_1 \bar{V}_1}{C_3 \bar{V}_3}\right)\frac{\partial \mu_1}{\partial C_1} + \frac{C_2 \bar{V}_1}{C_3 \bar{V}_3}\frac{\partial \mu_2}{\partial C_1}$$

$$b = \frac{C_1 \bar{V}_2}{C_3 \bar{V}_3}\frac{\partial \mu_1}{\partial C_1} + \left(1 + \frac{C_2 \bar{V}_2}{C_3 \bar{V}_3}\right)\frac{\partial \mu_2}{\partial C_1}$$

(26)

c and d are the same respectively as a and b except that

$\partial/\partial C_1$ is replaced by $\partial/\partial C_2$. In the range of validity of Henry's law, the thermodynamic quantities [41] can be evaluated by

$$\left(\frac{\partial \mu_1}{\partial C_1}\right)_{C_2} = RT\left[\left(\frac{\partial(\ln \gamma_1)}{\partial C_1}\right)_{C_2} + \frac{1}{C_1}\right.$$

$$\left. - \frac{1}{C_T} \times \left(1 - \frac{\bar{V}_1}{\bar{V}_3}\right)\right]$$

$$= RT\left[\frac{1}{C_T}\varepsilon_1^{(1)} + \frac{1}{C_1} - \frac{1}{C_T} \times \left(1 - \frac{\bar{V}_1}{\bar{V}_3}\right)\right]$$

$$= RT\left[\left(\frac{\partial(\ln \gamma_1)}{\partial C_2}\right)_{C_1} - \frac{1}{C_T} \times \left(1 - \frac{\bar{V}_2}{\bar{V}_3}\right)\right]$$

$$= RT\left[\frac{1}{C_T}\varepsilon_1^{(2)} - \frac{1}{C_T} \times \left(1 - \frac{\bar{V}_2}{\bar{V}_3}\right)\right]$$

where $C_T = C_1 + C_2 + C_3$. The values of $(\partial\mu_2/\partial C_2)_{C_1}$ and $(\partial\mu_2/\partial C_1)_{C_2}$ can be obtained by similar equations.

The phenomenological coefficients [42, 43] can be calculated by

$$L_{11} = \frac{C_1}{RT} D_1^*$$

(29)

and

$$L_{12} = -\frac{CN_1N_2}{RT}[N_2 D_1^* + N_1 D_2^*$$

$$+ N_3(D_1^* + D_2^* - D_3^*)]$$

(30)

where D_1^*, D_2^* and D_3^* are the impurity diffusion coefficients of the ternary alloys and C is the mean molar density. Although no impurity diffusion data are available for the Cu–Zn–Sn system, it is seen from the interdiffusion coefficients and mobilities of this work that the signs of L_{ii} must be positive and those of L_{ij} are negative. The results obtained at the selected compositions are listed in Table IV. The indirect coefficients L_{12} and L_{21} are smaller than the direct coefficients L_{11} and L_{22} but cannot be neglected. The Onsager reciprocal relation $L_{12} = L_{21}$ is again well verified.

4. Summary

The interdiffusion coefficients in the α f c c phase of Cu–Zn–Sn alloys, $\tilde{D}_{SnSn}^{Cu}$, $\tilde{D}_{SnZn}^{Cu}$, $\tilde{D}_{ZnZn}^{Cu}$ and $\tilde{D}_{ZnSn}^{Cu}$, have been determined at 1073 K. All of the four interdiffusion coefficients are positive and they are very sensitive to the solute concentrations. The interaction energy of the Cu–Sn bonds is much larger than the value for the Zn–Sn bonds. The results of the present work suggest

TABLE IV Phenomenological coefficients in α-Cu–Zn–Sn alloys at 1073 K

Composition (at %)		Phenomenological coefficient $(10^{-14}\,\text{mol}^2\,\text{J}^{-1}\,\text{m}^{-1}\,\text{sec}^{-1})^*$			
Zn	Sn	L_{11}	L_{22}	L_{12}	L_{21}
3.9	3.5	8.2	4.3	-0.20	-0.31
4.6	4.0	12	7.6	-1.1	-0.94
4.4	3.9	10	6.4	-0.44	-0.66
3.7	2.2	3.9	2.6	-0.14	-0.13
5.7	1.3	1.9	3.8	-0.077	-0.068
4.5	1.2	1.7	2.6	-0.17	-0.15

$^*1 \equiv$ Sn, $2 \equiv$ Zn, $3 \equiv$ Cu.

that the Onsager reciprocal relation is valid in the α phase field of the Cu–Zn–Sn system.

Acknowledgement

References

1. Y. MURAKAMI and K. KAMEI, "Materials of Nonferrous Metals" (Asakura Syoten, Tokyo, 1978) p. 29.
2. K. HIRANO, *Bull. Jpn Inst. Met.* **24** (1967) 856.
3. *Idem,* "Fundamentals and Application of Diffusion", edited by M. Doyama (Japan Institute of Metals, Sendai, 1984).
4. R. N. RHINES, R. A. MEUSSNER and R. T. DEHOFF, *Trans. Met. Soc. AIME* **242** (1968) 885.
5. J. S. KIRKALDY, B. J. BRIGHAM and D. H. WEICHERT, *Acta Metall.* **13** (1965) 885.
6. M. A. DAYANANDA, R. F. KIRSCH and R. E. GRACE, *Trans. Met. Soc. AIME* **242** (1968) 885.
7. K. YAMAGUCHI and I. NAKAMURA, *Rikagaku Kenkyusho Iho* **11** (1932) 1330.
8. J. B. MURPHY, *Acta Metall.* **9** (1961) 563.
9. I. UCHIYAMA, A. WATANABE and S. KIMOTO, "X-ray Micro Analyzer" (Nikkan Kogyo Newspaper Co., Tokyo, Japan, 1974) p. 127.
10. Y. TEZUKA and A. KAMIO, *J. Jpn Inst. Light Met.* **34** (1984) 301.
11. A. G. GUY, V. LEROY and T. B. LINDERMER, *Trans. ASM* **59** (1966) 517.
12. J. S. KIRKALDY, J. E. LANE and G. R. MASSON, *Can. J. Phys.* **41** (1963) 2174.
13. J. S. KIRKALDY, *ibid.* **35** (1957) 435.
14. T. TAKAHASHI, M. KATO, Y. MINAMINO and T. YAMANE, *Trans. Jpn Inst. Met.* **26** (1985) 462.
15. *Idem, Z. Metallkde* **74** (1983) 727.
16. *Idem, Met. Sci.* **18** (1984) 1333.
17. Y. MINAMINO, T. YAMANE, K. TSUKAMOTO, J. TAKAHASHI and H. KIMURA, *Trans. Jpn Inst. Met.* **25** (1984) 42.
18. T. TAKAHASHI, M. KATO, Y. MINAMINO and T. YAMANE, *J. Jpn Inst. Met.* **50** (1986) 243.
19. *Idem, J. High Temp. Soc. Jpn* **12** (1986) 98.
20. W. B. PEARSON, "A Handbook of Lattice Spacings and Structures of Metals and Alloys" (Pergamon, New York, 1958) p. 614.
21. A. VIGNES and C. E. BIRCHENALL, *Acta Metall.* **16** (1968) 1117.
22. J. KUCERA and B. MILLION, *Met. Trans.* **1** (1970) 2603.
23. A. M. BROWN and M. F. ASHBY, *Acta Metall.* **28** (1980) 1085.
24. D. B. BUTRYMOWICZ, J. R. MANNING and M. E. READ, "Incra Monograph V: The Metallurgy of Copper, Diffusion Rate Data and Mass Transport Phenomena for Copper Systems" (Institute for Materials Research, National Bureau of Standards, Washington, DC, 1977) p. 678.
25. J. S. KIRKALDY, D. WEICHERT and ZIA-UL-HAQ, *Can. J. Phys.* **41** (1963) 2166.
26. J. S. KIRKALDY, in "Isothermal Diffusion in Multicomponent Systems", edited by H. Herman (Interscience, New York, 1970) p. 60.
27. T. R. HEYWARD and J. I. GOLDSTEIN, *Met. Trans.* **4** (1973) 2335.
28. G. W. ROPER and D. P. WHITTLE, *Met. Sci.* **14** (1980) 21.
29. F. O. SHUCK and H. L. TOOL, *J. Phys. Chem.* **67** (1963) 540.
30. L. D. HALL, *J. Chem. Phys.* **21** (1953) 87.
31. A. VIGNES and J. P. SABATIER, *Trans. AIME* **245** (1969) 1795.
32. M. HANSEN and K. ANDERKO, "Constitution of Binary Alloys", 2nd Edn (McGraw-Hill, New York, 1958) p. 633.
33. K. HOSHINO, Y. IIJIMA and K. HIRANO, *Trans. Jpn Inst. Met.* **21** (1980) 674.
34. K. J. ANUSAVICE and R. T. DEHOFF, *Met. Trans.* **8A** (1972) 1279.
35. M. A. DAYANANDA, *Trans. Met. Soc. AIME* **242** (1968) 1369.
36. J. S. KIRKALDY, ZIA-UL-HAQ and L. C. BROWN, *ASM Trans. Q.* **56** (1963) 834.
37. A. BRUNSCH and S. STEEB, *Z. Metallkde* **65** (1974) 765.
38. T. O. ZIEBOLD and R. E. OGILVIE, *Trans. AIME* **239** (1967) 942.
39. D. D. FITTS, "Nonequilibrium Thermodynamics" (McGraw-Hill, New York, 1962) p. 104.
40. D. G. MILLER, *Chem. Rev.* **60** (1960) 15.
41. T. K. KETT and D. K. ANDERSON, *J. Phys. Chem.* **73** (1969) 1268.
42. K. NAGATA and K. S. GOTO, *J. Electrochem. Soc.* **123** (1976) 1814.
43. J. S. KIRKALDY and J. E. LANE, *Can. J. Phys.* **44** (1966) 2059.